HHS Public Access

Author manuscript

Biochim Biophys Acta Mol Cell Biol Lipids. Author manuscript; available in PMC 2024 January 26.

Published in final edited form as:

Biochim Biophys Acta Mol Cell Biol Lipids. 2022 August ; 1867(8): 159161. doi:10.1016/j.bbalip.2022.159161.

Ribosomal Targeting Strategy and Nuclear Labeling to Analyze Photoreceptor Phosphoinositide Signatures

Ammaji Rajala[1,4], **Rahul Rajala**[3,5], **Kenneth Teel**[1,4], **Raju V.S. Rajala**[1,2,3,4,*]

[1]Department of Ophthalmology, University of Oklahoma Health Sciences Center, Oklahoma City, OK, USA

[2]Department of Physiology, University of Oklahoma Health Sciences Center, Oklahoma City, OK, USA

[3]Department of Cell Biology, University of Oklahoma Health Sciences Center, Oklahoma City, OK, USA

[4]Dean McGee Eye Institute, Oklahoma City, OK, 73014 USA

[5]Cardiovascular Biology Program, Oklahoma Medical Research Foundation, Oklahoma City, OK, 73014 USA

Abstract

Reversible phosphorylation of phosphatidylinositol by phosphoinositide (PI) kinases and phosphatases generates seven distinct phosphoinositide phosphates, called phosphoinositides or PIPs. All seven PIPs are formed in the retina and photoreceptor cells. Around 50 genes in the mammalian genome encode PI kinases and PI phosphatases. There are no studies available on the distribution of these enzymes in the retina and photoreceptors.

Aim: To employ Ribosomal Targeting Strategy and Nuclear Labeling to Analyze Phosphoinositide Signatures in rod-photoreceptor cells.

Methods: HA-tagging of ribosomal protein *Rpl22* was induced with Cre-recombinase under the control of the rhodopsin promoter. Actively translating mRNAs associated with polyribosomes were isolated by immunoprecipitation with HA antibody, followed by RNA isolation and gene identification. We also isolated biotinylated-rod nuclei from NuTRAP mice under the control of the rhodopsin-Cre promoter and analyzed nuclear phosphoinositides.

Results: Our results indicate that the expression of class I and class III PI 3-kinase, PI4K IIIβ, PI 5-kinase, PIKfyve, PI3-phosphatases, MTMR2, 4, 6, 7, 14, PI4-phosphatase, TMEM55A,

[*]**Contact information:** Raju V.S. Rajala, Ph.D., 608 Stanton L. Young Blvd., Oklahoma City, OK 73104, Telephone: 405-271-8255, Fax: 405-271-8128, raju-rajala@ouhsc.edu.

Declaration of competing interest

The authors declare that they have no known competing financial interests or personal relationships that could have appeared to influence the work reported in this paper.

CRediT authorship contribution statement

RVSR conceived and supervised the study and wrote the manuscript. RVSR designed the research. RVSR, KT, and AR performed experiments. RR designed the primers, carried out all statistical analyses, and prepared the Venn diagrams.

Appendix A. Supplementary data

Included in this manuscript.

PI 5-phosphatases, SYNJI, INPP5B, INPP5E, INPP5F, SKIP and other phosphatases with dual substrate specificity, PTPMT1, SCAM1, and FIG4 are highly enriched in rod photoreceptor cells compared with the retina and cone-like retina. Our analysis identified the presence of PI(4)P, $PI(3,4)P_2$, $PI(3,5)P_2$, and $PI(4,5)P_2$ in the rod nuclei.

Conclusions: Our studies for the first time demonstrate the expression of PI kinases, PI phosphatases, and nuclear PIPs in rod photoreceptor cells. The NuTRAP mice may be useful not only for epigenetic and transcriptomic studies but also for *in vivo* cell-specific lipidomics research.

Keywords

Phosphoinositides; photoreceptor cells; retina; retinal degeneration; phosphoinositide kinases; phosphoinositide phosphatases; nuclear phosphoinositides; actively translating mRNAs

1. Introduction

Phosphoinositides constitute a minor fraction (~0.5-1%) of the total pool of phospholipids, but their functions in the cellular processes are indispensable [1-4]. The parent molecule phosphatidylinositol (PI) contains a D-*myo*-inositol head group and a glycerol backbone and two fatty acids are linked at the C1 and C2 positions of glycerol [1-3]. The inositol-head group of PI undergoes phosphorylation and generates distinct phosphatidylinositol phosphates, or PIPs [1-3]. PIPs are second messenger signaling molecules that directly interact with cytosolic or membrane proteins through PIP binding domains, which allows for membrane recruitment of proteins [2, 5]. Reversible phosphorylation of PI at the free-hydroxyl groups at the 3, 4, and 5 positions of its myo-inositol head group by phosphoinositide (PI) kinases and PI phosphatases generates seven distinct PIPs [1, 5]. These PIPs regulate numerous cellular functions, including vesicular transport, ciliogenesis, signal transduction, membrane budding and fusion, and cytoskeletal assembly [1-3]. Alterations in the expression and activity of PI kinases and PI phosphatases have been implicated in various diseases, including retinal degeneration [1-3, 6].

The retina is composed of several layers of neurons interconnected by synapses and is supported by an outer layer of pigmented epithelial cells that provides nutrients to the retina. There are seven types of neurons in the retina: rod photoreceptor cells, cone photoreceptor cells, bipolar cells, amacrine cells, horizontal cells, Müller cells, and ganglion cells [7]. In the retina, PI production and most of the enzymes that generate PIPs are light-dependently regulated [8-12]. Photoreceptors are light-sensing neuroepithelial cells, and PIPs have been shown to modulate channel modulation [13, 14], protein trafficking [15, 16], phototransduction [17, 18], and ciliogenesis [6]. The seven distinct PIPs are generated by the action of PI 3-kinases, PI 4-kinases, PI 5-kinases, PI 3-phosphatases, PI 4-phosphatases, and PI 5-phosphatases [1]. Although the PI kinases and PI phosphatases are broadly grouped into six categories (three kinases and three phosphatases), these enzymes exist in different forms; the PI 3-kinases are regulated by different regulatory subunits [19]. Because of this complexity, it is difficult to identify how a PIP signal is regulated in physiology and dysregulated in pathology. Furthermore, the regulatory and catalytic subunits of PI kinases may be differentially expressed in various retinal cell types. Around 50 genes

in the mammalian genome have been shown to encode PI kinases and PI phosphatases that regulate PI metabolism [19]. Thus, it is important to understand the unique and overlapping roles of PI kinases and PI phosphatases. This understanding is critical for our knowledge of both normal physiology and retinal pathology whose etiologies implicate the dysfunction of these proteins [2, 3]. One of the major limitations is the lack of antibodies to examine their endogenous expression in mammalian cells, including the retina. Some PI kinases and PI phosphatases have been identified through a proteomic study of mouse retina, but this approach lacks cell specificity [19]. Another method of identifying the PI kinases and PI phosphatases is single-cell RNA sequencing, which induces changes to gene expression that result from tissue dissociation and delays during cell sorting. This technique is limited, as RNA transcription may not reflect protein translation.

Nuclear phosphoinositides play an important role in cell survival, proliferation, and differentiation; their levels have been shown to increase in response to genotoxic and oxidative stress [20]. Photoreceptors live in a hostile oxidative environment; however, there are no studies to date on the nuclear phosphoinositide profile in rod photoreceptors. Isolated intact-rod nuclei are frequently contaminated with cone photoreceptors, as both have the same buoyancy and hamper enrichment of pure nuclei (author's unpublished data). To overcome this, we bred NuTRAP mice with mice expressing Cre-recombinase under the control of rhodopsin promoter, which labels the rod nuclei with biotin. Rod cell nuclear phosphoinositides were identified with the use of streptavidin affinity isolation of biotinylated-rod nuclei.

In the present study, we employed a novel and innovative *in vivo* method to isolate actively translating mRNAs of PI kinases and PI phosphatases from rod photoreceptor cells using RiboTag mice, and we compared the expression in rod photoreceptor cells with that in the total retina and cone-like retina $Nrl^{-/-}$ mouse retina [21]. We believe this approach balances the limitations of whole tissue proteomics and single-cell RNAseq, as we have the specificity and resolution to identify alterations in a single cell type, as well as bridging the gap between RNA and protein by identifying actively translating mRNA. The NuTRAP mice may be useful not only for epigenetic and transcriptomic studies but also for *in vivo* cell-specific lipidomics research.

2. Materials and Methods

2.1. Animals

All animals were treated in accordance with the *ARVO Statement for the Use of Animals in Ophthalmic and Vision Research* and the *NIH Guide for the Care and Use of Laboratory Animals.* The protocols were approved by the IACUC at the University of Oklahoma Health Sciences Center. Breeding pairs of RiboTag (Jax #011029) and NuTRAP (Nuclear tagging and Translating Ribosome Affinity Purification) (Jax # #029899) mice were purchased from The Jackson Laboratory (Bar Harbor, Maine). The $Nrl^{-/-}$ mice were kindly provided by Dr. Anand Swaroop (NIH, Bethesda, MD). The rhodopsin-Cre (i75Cre) mice have been described earlier [22] and were provided by Dr. Ching-Kang Jason Chen (Baylor College of Medicine, Houston, TX). Animals were born and raised in our vivarium and kept under dim cyclic light (40-60 lux, 12 h light/dark cycle). All mice were screened for *rd1* and

rd8 mutations and were negative for these mutations. The mice were deeply anesthetized, and the retinas were harvested. The mice were euthanized by CO_2 asphyxiation. The retinas were used for RNA and nuclei isolation, or enucleated eyes were used for immunohistochemistry.

2.2. Generation of conditional rod-specific RiboTag mice

The RiboTag mouse carries a ribosomal protein gene (*Rpl22*) with a floxed C-terminal exon followed by an identical exon tagged with hemagglutinin (HA) epitope [23]. We bred RiboTag mice with mice carrying Cre-recombinase under the control of a rhodopsin promoter [22]. The desired transgenic mice were identified by genotyping of tail DNA for Cre and floxed HA, using PCR screening. To identify rhodopsin-*cre*, PCR was performed with genomic DNA and sense (5'- TCAGTGCCTGGAGTTGCGCTGTGG −3') and antisense (5'-CTTAAAGGCCAGGGCCTGCTTGGC-3') primers to amplify a 500-bp product. To identify HA floxed alleles, we used sense (5'- GGGAGGCTTGCTGGATATG-3') and antisense (5'- TTTCCAGAC ACAGGCTAAGTACAC-3') primers to amplify genomic DNA by PCR. The wild-type allele generates a 243-bp product, the heterozygous allele generates 290-bp and 243-bp products, and the homozygous HA allele generates a 290-bp product.

2.3. Isolation of polyribosomes containing actively translating mRNAs

Using a modified method from Cleuren et al. [24], we isolated polyribosomes containing actively translating mRNAs. Retinas from two mice (2-to-4-months-old) were removed and placed in a DMEM medium containing cycloheximide (100 μg/mL) and incubated for 10 min. Then, the retinas were flash-frozen in liquid nitrogen and pulverized with a hand homogenizer. The powder was resuspended in 200 μl of polysome buffer (50 mM Tris-HCl [pH 7.5], 100 mM KCl, 12 mM $MgCl_2$, 1% Igepal CA-630, 1 mM dithiothreitol, 200 U/mL RnaseOUT, 1 mg/mL heparin sodium salt, 100 μg/mL cycloheximide plus EDTA-free protease inhibitor cocktail in DEPC water), mixed by pipetting, and centrifuged at 15,000 RPM at 4 °C. The clear lysate was incubated with a purified mouse monoclonal HA antibody (5 μl/200 μl lysate) for 1 hour at 4 °C. Magnetic protein G beads, equilibrated in polysome buffer, were added to the retinal lysate containing HA antibody. Beads were then incubated for an additional 30 min at 4 °C. The magnetic beads containing immune-complexes were washed three times with high salt buffer (50 mM Tris-HCl [pH 7.5], 300 mM KCl, 12 mM $MgCl_2$, 1% Igepal CA-630, 1 mM dithiothreitol, 200 U/mL RnaseOUT, 1 mg/mL heparin sodium salt, 100 μg/mL cycloheximide plus EDTA-free protease inhibitor cocktail). To the beads, we added 500 μl of TRIzol and isolated RNA using a PureLink RNA Mini Kit (Ambion, Carlsbad, CA). First-strand cDNA was synthesized using the Superscript III first-strand synthesis kit (Invitrogen).

2.4. Generation of rod-specific NuTRAP mice

The NuTRAP (Nuclear tagging and Translating Ribosome Affinity Purification) allele has a *loxP*-flanked STOP sequence preventing transcription of three individual components: BirA, BLRP-tagged mCherry/mRANGAP1, and EGFP/L10a [25]. When expressed, the BLRP-tagged mCherry/mRANGAP1 protein is biotinylated by BirA, allowing for nuclear membrane labeling with mCherry and biotin (which enables nuclear isolation by either

fluorescence- and/or affinity-based purification). Furthermore, EGFP/L10a fluorescently tags the translating mRNA polysome complex, which enables the isolation of RNAs that are actively engaged by ribosomes, or the isolation of intact cells by fluorescence purification. In combination with tissue- or cell-specific Cre-recombinase, the NuTRAP mice allow the labeling and simultaneous isolation of cell type-specific nuclei and mRNA within a heterogeneous tissue.

We bred NuTRAP mice with mice expressing Cre-recombinase under the control of rhodopsin promoter. The desired transgenic mice were identified by genotyping of tail DNA for Cre and floxed HA, using PCR screening. To identify rhodopsin-*cre*, PCR was performed with genomic DNA and sense (5'- TCAGTGCCTGGAGTTGCGCTGTGG −3') and antisense (5'- CTTAAAGGCCAGGGCCTGCTTGGC-3') primers to amplify a 500-bp product. To identify NuTRAP floxed alleles, we used sense (5'- AGGACGGCGAGTTCATCTAC-3') and antisense (5'- TGGTGT AGTCCTCGTTGTGG-3') and internal positive control sense (5'- CAAATGTTGCTTGTCTGG TG-3') and antisense (5'- GTCAGTCGAGTGCACAGTTT-3') primers to amplify genomic DNA by PCR. The wild-type allele generates a 200-bp product, the heterozygous allele generates 200-bp and 288-bp products, and the homozygous allele generates a 288-bp product.

2.5. Isolation of biotinylated-rod nuclei

Retinas were harvested from heterozygous NuTRAP mice carrying a Cre-recombinase under the control of rhodopsin promoter and Cre-negative littermates. We isolated nuclei from mouse retina via a method used for isolation of intact rat liver nuclei [26] with modifications. All procedures were carried out at 4 °C. Retinas were harvested from six mice (2-months-old) and then homogenized in 0.32M sucrose containing 3 mM $MgCl_2$. The homogenate was diluted with water to a final concentration of 0.25M sucrose. We pelleted the crude nuclei by ultracentrifugation at 700 x g for 10 min. The pellet was resuspended in 13 ml of 0.25M sucrose containing 1 mM $MgCl_2$ and centrifuged at 50,000 x g for 60 min at 4 °C. During this spin, the nuclei sedimented to the bottom of the tube, whereas the contaminating erythrocytes, whole cells, and mitochondria floated as a plug at the top of the tube and were removed with a spatula. The pellet was resuspended in 250 μl nuclei purification buffer (NPB: 20 mM HEPES [pH 7.5], 40 mM NaCl, 90 mM KCl, 2 mM EDTA, 0.5 mM EGTA, and protease inhibitor cocktail) and passed through a 70 Micron Cell Strainer (Catalog #13680-0070, Certified MTP) attached to a 1.0-ml pipette tip. The nuclei sample was assessed using a BioRad cell counter. Thirty microliters of M-280 Streptavidin Dynabeads (#11205, ThermoFisher Scientific) were transferred to a 1.5-ml Eppendorf tube and washed three times with NPB using DynaMag2 Magnet (#12321; ThermoFisher Scientific). The washed beads were gently mixed with the nuclear suspension and incubated at 4 °C for 40 min under gentle rotation. The streptavidin-bound nuclei were magnetically separated with the DynaMag2 Magnet and washed in the magnet three times. To the washed beads, we added 2 ml of chloroform: methanol (1:2) and extracted phosphoinositides.

2.6. Extraction and analysis of phosphoinositides

Phosphoinositides were extracted according to the method we described earlier [27]. Lipid phosphorous was measured and converted to phospholipid (PL) [27, 28]. Phosphoinositide levels were measured by plating 1000 pmols of PL and an ELISA assay was carried out using phosphoinositide probes [27, 28]. We measured six phosphoinositides using probes: 2 X Hrs for PI(3)P, FAPP1for PI(4)P, TAPP1 for PI(3,4)P_2, Svp1p (PI,3,5)P_2, PLCδ for PI(4,5)P_2, and Grp1 for PI(3,4,5)P_3. The PI(3,5)P_2 probe, Svp1p [29], was obtained from Echelon Biosciences (Salt Lake City, UT). We measured the levels of PIPs from streptavidin-bound nuclei from NuTRAP control and NuTRAP/Cre mouse retinas. Relative levels of PIPs were calculated by subtracting the controls from NuTRAP/Cre data.

2.7. Quantitative Real-Time Reverse Transcription Polymerase Chain Reaction

The PCR reaction contains 3.2 nmol first-strand cDNA, 3 pmol sense and antisense primers, and Eva green supermix (Bio-Rad). A final volume of 12 μl was used for each sample. The primers used for the amplification of retina cell-specific markers, PI kinases, and PI phosphatases are listed in Tables 1-3. The PCR was carried out on a CFX96™ Real-Time System and C1000 Touch Thermal Cycler (Bio-Rad). Fluorescence changes were monitored after each cycle (SYBR Green). Melting curve analysis was performed (0.5 °C/s increase from 55 to 95 °C with continuous fluorescence readings) at the end of 48 cycles to ensure that specific PCR products were obtained. All reactions were performed in triplicate. The average CT (threshold cycle) of fluorescence units was used for analysis. Each mRNA level was normalized by the actin levels. Quantification was calculated using the CT of the target signal relative to the actin signal in the same RNA sample. The genes that yielded CT values greater than 36 were considered low yield and were excluded from the final analysis.

2.8. R Venn diagram analysis

Using results from volcano plots, phosphoinositide-converting genes with significant changes ($p<0.05$) in *Rpl22* mice and cone-like *Nrl*$^{-/-}$ mice were tabulated by whether they were enriched or depleted. Genes were listed in a CSV file (Supplementary Table 1), which was then imported into an R data frame. Venn diagrams were then created using the Venn diagram library in the R programming language. Set algebra functions (Intersect) were also used to identify commonly enriched and depleted genes between *Rpl22* mice and cone-like *Nrl*$^{-/-}$ mice.

3. Results

3.1. Phosphoinositide lipids

The parent phosphatidylinositol (PI) molecule undergoes phosphorylation by PI 3-kinases, PI 4-Kinases, and PI 5-kinases. These phosphorylation products are dephosphorylated by PI 3-phosphatases, PI 4-phosphatases, and PI 5-phosphatases to generate seven distinct phosphoinositides (Fig. 1). These lipids are PI(3)P, PI(4)P, PI(5)P, PI(3,4)P_2, PI(3,5)P_2, PI(4,5)P_2, and PI(3,4,5)P_3. These seven PIPs can be interconverted through the action of PI kinases and PI phosphatases (Fig. 1, Tables 4 and 5).

3.2. Rod-specific expression of HA-tagged ribosomes

The RiboTag mouse carries a ribosomal protein gene, *Rpl22*, with the floxed C-terminal exon 4 followed by an identical exon 4 tagged with hemagglutinin (HA) [23]. When RiboTag mice are crossed with mice expressing cell-specific Cre-recombinase, the alternative HA-epitope-tagged exon is incorporated into the *Rpl22* gene in a cell-specific manner [23]. Our data show that the breeding of rhodopsin-Cre mice with *Rpl22* floxed mice (abbreviated as $^{rod}Rpl22^{+/0}$) resulted in the expression of HA-tagged ribosomal protein in the rod inner segments (Fig.2A-C). Polyribosomal immunoprecipitation (IP) with HA antibody recovered ribosomal-associated mRNA (Fig. 2D). The RNA recovered from rhodopsin-Cre/ *Rpl22* gave a concentration of 30 ng/μl; qRT-PCR analysis of mRNA with cell-specific markers [30]: rod- (rhodopsin, PDE6A), retinal pigment epithelium- (RPE65), cone- (OPN1SW), retinal ganglion cell- (SNCG), bipolar cell- (TMEM215), amacrine cell- (GAD1), horizontal cell- (ONECUT1), Müller glia- (GFAP), microglia and astrocyte- (C1QA), and vascular cell- (RGS5) specific primers showed the enrichment of only rod-specific transcripts and the depletion of all other retinal cell types (Fig. 2E). These studies confirm rod-cell-specific isolation of actively translating mRNAs. Prior studies have demonstrated that rods constitute 40% of the total cells in the retina [31]. Our RiboTag recovery of rod-specific transcripts yielded 3-4-fold enrichment. A 3-fold increase is roughly what one would expect if rods did constitute 40% of total retina transcripts, further validating our approach and sample quality.

3.3. Interpretation of the data.

All studies are done on mRNA levels. Therefore, we described higher expression; this means that there is a greater enrichment of the transcript in our HA-IP pull-downs. When we describe lower expression, this means that there is a depletion of the transcript in the HA-IP pull-down. Depletion may not necessarily mean the respective PI kinase or PI phosphatase is absent in the cell, just that the predominant source of transcript is coming from a different cell type(s). Furthermore, we compared the data between retina and cone-like ($Nrl^{-/-}$ mouse retina). Mouse retina is rod-dominant retina containing 95% rods and <5% cones [32, 33]. If a protein(s) is expressed in both rods and cones, it is difficult to identify protein changes in cones due to rod dominance. Neural retina leucine zipper transcription factor (*Nrl*) plays an essential role in rod photoreceptor differentiation and homeostasis [21]. The $Nrl^{-/-}$mouse retina does not form rods, but is populated with cone-like photoreceptors, which are histochemically, molecularly, and ultrastructurally indistinguishable from wild-type cones [34]. Moving forward in the rest of the text, we will make comparisons between wild-type retina and rods, as well as wild-type retina and cones. However, when referring to cones, we are referring to a cone-like retina. All changes are compared back to the wild-type retina.

3.4. PI 3-kinases in rods and cones

The PI 3-kinases are broadly classified into three categories: class I, class II, and class III PI3Ks [1, 2]. Class I PI3Ks are heterodimeric proteins composed of catalytic and regulatory subunits. The catalytic subunits of class I PI3K, p110α, p110β, and p110γ, were significantly enriched in rods compared with the retina and cones (Fig. 3A); however, the expression of p110γ was substantially reduced in the cones (Fig. 3A). Class II PI3Ks PI3K-

C2α and PI3K-C2β were expressed in rods; however, the expression of PI3K-C2γ was significantly lower in rods than in the retina and cones (Fig. 3A). The class II PI3K-enzymes PI3K-C2α and PI3K-C2γ were higher in cones than in the retina (Fig. 3A).

The class III PI3K Vps34 was significantly enriched in rods compared with retina and cones (Fig. 3A). The regulatory subunits of class I PI3K p85β and class III PI3K Vps15 were significantly enriched in rods compared within the retina and cones (Fig. 3A). The expression of p85α, the regulatory subunit of class I PI3K, was significantly lower in rods, whereas the expression of p101 and p87 were almost negligible in rods compared with the retina and cones (Fig. 3A). The expression of PI3K-inhibitory protein PI3KIP1 was significantly lower in rods and cones than in the retina (Fig. 3A). These observations suggest that components of class I and class III PI3K signaling are present at higher levels in rods compared with components of class II PI3K signaling.

3.5. PI 4-kinases in rods and cones

PI4K IIα, PI4K IIβ, and PIK4K IIIβ were expressed in rods; however, the level of PI4K IIIβ was enriched in rods than in the retina and cones (Fig. 4B). There was no PI4K IIIα expression in rods, and cones expressed significantly higher levels of PI4K IIβ (Fig. 4B). These observations suggest that PI4K IIIβ may be the major PI4K in rods.

3.6. PI 5-kinases in rods and cones

Type I PIPKs catalyze the phosphorylation of PI(4)P to PI(4,5)P_2. There are three members of this family: PIPK 1α, PIPK 1β, and PIPK 1γ. Type II PIPKs catalyzes the phosphorylation of PI(5)P to PI (4,5)P_2, and there are three members of this family: PIPK IIα, PIPK IIβ, and PIPK IIγ. Rods expressed PIPK Iα, PIPK Iγ, PIPK IIα, PIPK IIγ, and PIKFyve (Fig. 3C). The expression of PIPK 1β was lower in rods than in the retina and cones, whereas the expression of PIPK IIβ was absent from rods (Fig. 3C). PIKFyve is a type III PIPK that phosphorylates PI to PI (5)P. PIKFyve also phosphorylates PI(3)P to PI (3,5)P_2. Interestingly, PIKFyve was expressed more highly than other PI 5-kinases in rods (Fig. 3C), suggesting that it may be the major PI 5-kinase in rods.

3.7. PI 3-phosphatases in rods and cones

We found the expression of PTEN, MTM1, MTMR2, MTMR3, MTMR4, MTMR5, MTMR6, MTMR7, and MTMR14 in rods. Among these PI 3-phosphatases, MTMR2, MTMR3, MTMR4, MTMR6, MTMR7, and MTMR14 expression levels were enriched in rods compared with retina and cones (Fig, 3D). Compared with the other PI 3-phosphatases in rods, the expression level of MTM1 was lower, whereas MTMR8 levels were undetectable (Fig. 3D).

3.8. PI 4-phosphatases in rods and cones

PI 4-phosphatases, INPP4A, INPP4B, TMEM55A, and TMEM55B are expressed in rods, retina, and cones. Our results showed that TMEM55A expression was the only PI 4-phosphatase enriched in rods (Fig. 3E). The expression of INPP4A was significantly lower in rods and cones than in the retina (Fig. 3E), whereas the expression of INPP4B and TMEM55B was significantly lower in rods than in the retina and cones (Fig. 3E). These

observations suggest that TMEM55A may be the predominant PI 4-phosphatase in rods. However, the expression levels of TMEM55B were comparable between rods and cones (Fig. 3E).

3.9. PI 5-phosphatases in the rods- and cones

We found significantly increased expression of SYNJ1, INPP5B, INPP5E, INPP5F, and SKIP in rods compared with the retina and cones (Fig. 3F). The expression of SYNJ2 was lower in rods than in the retina and cones (Fig. 3F).

The other phosphatases, PIPMT1, SACM1, and FIG4, were also expressed in rods, and their levels were enriched in rods than in the retina and cones (Fig. 3G). These phosphatases have overlapping specificity with other PIPs. PTPM1 is able to dephosphorylate PIPs in the 3rd position and it has a preference for PI(5)P [35]. The expression of VAC14 was significantly higher in rods than in the retina and cones (Fig. 3G). VAC14 is a regulatory protein that forms a complex with PIKFyve and FIG4, and it regulates the generation of PI(3,5)P_2 [36]. Phosphatidylinositol transfer protein beta (PITPβ) is an important protein in PI metabolism, as it transfers PI and phosphatidylcholine (PC) across membranes [37]. The PITPβ expression was enriched in rods compared with the retina and cones (Fig. 3G).

3.10. Identification of rod-rich, rod-poor, cone-rich, and cone-poor transcripts

To identify transcripts enriched or depleted in rods versus cones, we generated volcano plots (Fig. 3H and I). Using the R programming language (source code in Supplementary File 1), we generated a Venn diagram (Fig. 3J) comparing the following four categories: (1) Cone-rich transcripts, which were significantly enriched in the cones; (2) Cone-poor transcripts, which were significantly decreased in the cones; (3) Rod-rich transcripts, which were significantly enriched in *Rpl22* isolates; and (4) Rod-poor transcripts, which were significantly decreased in *Rpl22* isolates (CSV file of enriched and depleted genes in the Supplementary Table 1). If a particular transcript is enriched in both rods and cones, this suggests that this transcript is enriched in rods. If a transcript is depleted in rods and cones, this finding suggests that this transcript is expressed to a greater extent in the non-photoreceptor cells of the retina. If a transcript is enriched in rods and simultaneously depleted in cones, this finding suggests that this transcript is specifically enriched in rods. The inverse suggests that the transcript is specifically enriched in cones. Using this approach, we identified phosphoinositide-converting enzymes that have differential expression between rods and cones and the total retina (Table 6).

3.11. Characterization of rod-specific NuTRAP mice

NuTRAP mice allow the labeling of nuclei with biotin and mCherry and labeling of ribosomes with GFP upon Cre-mediated recombination in a tissue- or cell-specific manner (Fig. 4A). We generated heterozygous NuTRAP mice in the presence ($^{rod}Nutrap^{+/0}$) or absence ($Nutrap^{+/0}$) of rhodopsin-Cre. Mouse retina sections were stained with GFP antibody and showed the expression of GFP in $^{rod}Nutrap^{+/0}$ mice, but not in Nutrap$^{+/0}$ mice (Fig. 4B-D). The GFP labeling is observed in rod inner segments where the protein synthetic machinery, including ribosomes, is localized. Mouse retina sections stained with mCherry antibody showed staining in the outer nuclear layer of $^{rod}Nutrap^{+/0}$ mice, but not in

Nutrap$^{+/0}$ mice (Fig. 4E-H). Immunoblot analysis further confirmed the expression of GFP, mCherry, and streptavidin in ^{rod}*Nutrap*$^{+/0}$ mice, but not in *Nutrap*$^{+/0}$ mice (Fig. 4I). These observations suggest that rod-Cre facilitates the labeling of nuclei with biotin and mCherry and ribosomes with GFP.

3.12. Determination of nuclear phosphoinositides

Biotinylated nuclei were affinity-purified with streptavidin-conjugated magnetic beads and the phosphoinositides were extracted. We used PI(3)P, PI(4)P, PI(3,4)P_2, PI(3,5)P_2, PI(4,5)P_2, and PI(3,4,5)P_3 lipid-binding probes to determine their levels in the nuclei (Fig. 4J). The data were compared with the total retina normalized to 1.0. PI(3)P and PI(3,4,5)P_3 were absent from the nuclei, and the relative levels of PI(3,4)P_2 and PI(4,5)P_2 were significantly lower in the nuclei (Fig. 4K). PI(4)P and PI(3,5)P_2 were present in the nuclei (Fig. 4K). We examined the levels of PI(3)P and PI(3,4,5)P_3 in mouse liver and mouse liver nuclei and found that these lipids were present in the nuclei (**Fig. 5L**). These observations suggest that NuTRAP mice can be used to isolate nuclei in a cell-specific manner to identify nuclear phosphoinositides.

4. Discussion

The RiboTag method to isolate actively translating mRNAs from rod photoreceptor cells provided an enormous amount of information concerning PI kinases and PI phosphatases. Our current study identified transcripts that are rod-rich/cone-poor, rod-poor/cone-rich, rod-/cone-rich, and rod-/cone-poor. The rod-rich/cone-poor and rod-poor/cone-rich transcripts in rods and cones suggest that phosphoinositide signaling could be different in rods and cones. Studying the functional roles of these PI kinases and PI phosphatases in rods and cones greatly advances our understanding of rod and cone photoreceptor biology. We could use NuTRAP instead of RiboTag mice for the isolation of actively translating mRNAs, as we found that HA-tagged antibody has more affinity to bring down HA-tagged ribosomes, as opposed to GFP-tagged ribosomes in the NuTRAP method.

Our earlier studies show that conditional deletion of the regulatory subunit of class I PI3K, p85α, in rods did not affect rod structure and function [38], but cone-specific deletion of p85α resulted in age-related cone-degeneration [39]. In line with the earlier studies, rods express higher levels of p85β and cones express higher levels of p85α. Consistent with the higher enrichment of class III PI3K catalytic (Vps34) and its regulatory subunit (Vps34) in rods, conditional deletion of Vps34 in rods has previously been shown to result in photoreceptor degeneration [11]. Our study further confirms that higher enrichment in these PI3K enzymes in rods and cones has functional relevance in photoreceptor biology. A novel observation from the present study is that rods highly express p110α, p110β, and p110γ catalytic subunits, and they may interact with p85β for its membrane localization. It is not clear why rods have this functional redundancy in the expression of PI3K catalytic subunits. Further studies are needed to establish whether they have any non-redundant roles in rod cells.

We found both PI4K IIα and PI4K IIIβ transcripts in rods. It appears that PI4K IIIβ may be the major PI4-kinase for the generation of PI(4)P in rods, which is essential for cilia

maintenance [40]. The rod outer segment is a modified sensory cilium and it is interesting to study the role of these PI4Ks in the context of retinal diseases that affect photoreceptors. Expression of the PI5-kinase PIKFyve is higher in rods, and this enzyme is regulated by two other proteins, a 5'phosphatase, FIG4, and a scaffold, Vac14 [41, 42]. In other cell types, loss of these proteins resulted in neurodegeneration [43]. Their roles in rods remain to be established. We found that FIG4 knockdown in rods resulted in photoreceptor degeneration (authors' unpublished data).

A striking feature noted in rods is the higher expression levels of various PI 3-phosphatases. It is important to understand why rods express numerous 3'-phosphatases, and their roles in photoreceptor biology are yet to be determined. In rods, PI(3)P is essential for endocytic trafficking [11], and dephosphorylation of this phosphoinositide could be detrimental. Further studies are needed as to how 3-phosphatases are controlled in rods to regulate endocytic trafficking. Rods predominantly express TMEM55A, which is also known as $PI(4,5)P_2$ 4-phosphatase [44]. Its role in rods is yet to be determined. The 4-phosphatase was initially identified in bacteria, and the generated PI(5)P from $PI(4,5)P_2$ has been shown to activate the PI3K/Akt pathway [45]. In photoreceptors, Akt activation is neuroprotective [46]. Conventionally, the PI(5)P is generated from PI by the phosphorylation of PI5-kinase, PIKFyve. The enriched levels of $PI(4,5)P_2$ 4-phosphatase in rods suggest the existence of an alternative pathway for the production of PI (5)P in rods. Studying the role of 4-phosphatase in rods not only helps us to understand the alternative source of PI(5)P but also how $PI(4,5)P_2$ levels are maintained in rods. This is especially important because $PI(4,5)P_2$ determines the length and stability of primary cilia by balancing membrane turnover [47]. Studying its role in photoreceptors will greatly advance our understanding since photoreceptor outer segments are modified sensory cilia.

Similar to PI3-phosphatases, rods express several PI 5-phosphatases. A recent study showed that ablation of INPP5E in the mouse retina impairs photoreceptor axoneme formation and prevents disc biogenesis [6]. Interestingly, in rods, the levels of INPP5B and INPP5F are much higher than are levels of INPP5E, and they also dephosphorylate the same substrates that INPP5E does. Therefore, it is curious why INPP5B cannot complement the lethal phenotypes of INPP5E in rods. Understanding the roles of these INPP5s would greatly advance our understanding of photoreceptor biology. Our study also highlighted the enrichment of skeletal muscle- and kidney-enriched inositol phosphatase (SKIP), mitochondrial phosphatase PTPMT1, and SACM1 in rods. Their roles in photoreceptor biology are yet to be determined.

In the present study, PITPβ expression is higher in rods. It has been shown previously that this protein regulates the cone outer segment integrity in the zebrafish retina [48] and promotes photoreceptor survival and recovery of light stimulation in *Drosophila* [49]. We recently reported that PITPβ interacts with βA3/A1-crystallin and this complex regulates $PI(4,5)P_2$ levels in the RPE [50]. The deficiency of βA3/A1-crystallin in RPE resulted in decreased ezrin phosphorylation, EGFR activation, internalization, and degradation [50]. However, the role of this protein in rods is yet to determined.

The NuTRAP method enabled us to measure nuclear PIPs in rod photoreceptor cells. The NuTRAP mice have been used to study cell-type-specific changes in epigenetic and transcriptomic profiles [25, 51]. Our studies suggest that this approach can be used for lipidomic research. Previous studies show that PIPs are present in the nucleus, and their levels increased in response to proliferative stimuli and genotoxic and oxidative stress [20]. The class I PI3K enzyme-generated product PI(3,4,5)P_3 is shown to be increased in response to proliferative stimuli [20], and we found the absence of PI(3,4,5)P_3 in rod nuclei. Photoreceptors are postmitotic cells, whereas the liver is mitotic tissue; we found PI(3)P and PI(3,4,5)P_3 in the liver nuclei. Furthermore, our data also show the significant enrichment of many PI-3 phosphatases; the nuclear localization of some of these phosphatases may prevent the formation of PI(3)P and PI(3,4,5)P_3. Further studies are needed to understand whether environmental and genetic stress in the retina alters the expression of nuclear PIPs. Nevertheless, we show in the present study that cell-specific nuclei can be isolated using NuTRAP mice and can be used for the analysis and identification of nuclear PIPs.

5. Conclusions

Our studies first time demonstrate the expression of PI kinases, PI phosphatases, and nuclear PIPs in rod photoreceptor cells. The NuTRAP mice may be useful not only for epigenetic and transcriptomic studies but for *in vivo* cell-specific lipidomics research. The data presented in this manuscript will help investigators further examine the functional roles of identified PI kinases and PI phosphatases in rod photoreceptor cells. This study will also inspire others to isolate actively translating mRNA and analyze nuclear PIPs from other retinal cells, including cones, bipolar cells, amacrine cells, horizontal cells, RPE cells, ganglion cells, and Müller cells, to compare cell-specific expression and changes in health and disease.

Supplementary Material

Refer to Web version on PubMed Central for supplementary material.

Acknowledgment

Grants from the National Institutes of Health (EY030024, EY00871, NEI Core grant EY12190), the BrightFocus Foundation, Inc., Oklahoma Center for Adult Stem Cell Research, and an unrestricted grant from Research to Prevent Blindness, Inc. The authors also acknowledge Ms. Kathy J. Kyler, Staff Editor, University of Oklahoma Health Sciences Center, for editing this manuscript.

References

[1]. Balla T, Phosphoinositides: tiny lipids with giant impact on cell regulation, Physiol Rev., 93 (2013) 1019–1137. [PubMed: 23899561]

[2]. Rajala RVS, Signaling roles of phosphoinositides in the retina, J Lipid Res, (2021) 100041. [PubMed: 32540927]

[3]. Wensel TG, Phosphoinositides in Retinal Function and Disease, Cells, 9 (2020) 866. [PubMed: 32252387]

[4]. Brockerhoff SE, Phosphoinositides and photoreceptors, Mol Neurobiol, 44 (2011) 420–425. [PubMed: 21928087]

[5]. Idevall-Hagren O, De Camilli P, Detection and manipulation of phosphoinositides, Biochim Biophys Acta, 1851 (2015) 736–745. [PubMed: 25514766]

[6]. Sharif AS, Gerstner CD, Cady MA, Arshavsky VY, Mitchell C, Ying G, Frederick JM, Baehr W, Deletion of the phosphatase INPP5E in the murine retina impairs photoreceptor axoneme formation and prevents disc morphogenesis, J Biol Chem, 296 (2021) 100529. [PubMed: 33711342]

[7]. Cepko C, Intrinsically different retinal progenitor cells produce specific types of progeny, Nature reviews. Neuroscience, 15 (2014) 615–627. [PubMed: 25096185]

[8]. Rajala RV, McClellan ME, Ash JD, Anderson RE, In vivo regulation of phosphoinositide 3-kinase in retina through light-induced tyrosine phosphorylation of the insulin receptor beta-subunit, J.Biol.Chem, 277 (2002) 43319–43326. [PubMed: 12213821]

[9]. Anderson RE, Hollyfield JG, Light stimulates the incorporation of inositol into phosphatidylinositol in the retina, Biochim.Biophys.Acta, 665 (1981) 619–622. [PubMed: 7295756]

[10]. Anderson RE, Maude MB, Kelleher PA, Rayborn ME, Hollyfield JG, Phosphoinositide metabolism in the retina: localization to horizontal cells and regulation by light and divalent cations, J.Neurochem, 41 (1983) 764–771. [PubMed: 6308171]

[11]. He F, Agosto MA, Anastassov IA, Tse DY, Wu SM, Wensel TG, Phosphatidylinositol-3-phosphate is light-regulated and essential for survival in retinal rods, Sci.Rep, 6 (2016) 26978. [PubMed: 27245220]

[12]. Huang Z, Anderson RE, Cao W, Wiechmann AF, Rajala RV, Light-Induced Tyrosine Phosphorylation of Rod Outer Segment Membrane Proteins Regulate the Translocation, Membrane Binding and Activation of Type II alpha Phosphatidylinositol-5-Phosphate 4-Kinase, Neurochem.Res, 36 (2011) 627–635. [PubMed: 20204506]

[13]. Bright SR, Rich ED, Varnum MD, Regulation of human cone cyclic nucleotide-gated channels by endogenous phospholipids and exogenously applied phosphatidylinositol 3,4,5-trisphosphate, Mol.Pharmacol, 71 (2007) 176–183. [PubMed: 17018579]

[14]. Brady JD, Rich ED, Martens JR, Karpen JW, Varnum MD, Brown RL, Interplay between PIP3 and calmodulin regulation of olfactory cyclic nucleotide-gated channels, Proc.Natl.Acad.Sci.U.S.A, 103 (2006) 15635–15640. [PubMed: 17032767]

[15]. Deretic D, Traverso V, Parkins N, Jackson F, Rodriguez de Turco EB, Ransom N, Phosphoinositides, ezrin/moesin, and rac1 regulate fusion of rhodopsin transport carriers in retinal photoreceptors, Mol.Biol.Cell, 15 (2004) 359–370. [PubMed: 13679519]

[16]. Lee SJ, Montell C, Light-dependent translocation of visual arrestin regulated by the NINAC myosin III, Neuron, 43 (2004) 95–103. [PubMed: 15233920]

[17]. Womack KB, Gordon SE, He F, Wensel TG, Lu CC, Hilgemann DW, Do phosphatidylinositides modulate vertebrate phototransduction?, J.Neurosci, 20 (2000) 2792–2799. [PubMed: 10751430]

[18]. He F, Mao M, Wensel TG, Enhancement of phototransduction g protein-effector interactions by phosphoinositides, J.Biol.Chem, 279 (2004) 8986–8990. [PubMed: 14699118]

[19]. Sasaki T, Takasuga S, Sasaki J, Kofuji S, Eguchi S, Yamazaki M, Suzuki A, Mammalian phosphoinositide kinases and phosphatases, Prog Lipid Res, 48 (2009) 307–343. [PubMed: 19580826]

[20]. Chen M, Wen T, Horn HT, Chandrahas VK, Thapa N, Choi S, Cryns VL, Anderson RA, The nuclear phosphoinositide response to stress, Cell Cycle, 19 (2020) 268–289. [PubMed: 31902273]

[21]. Mears AJ, Kondo M, Swain PK, Takada Y, Bush RA, Saunders TL, Sieving PA, Swaroop A, Nrl is required for rod photoreceptor development, Nat.Genet, 29 (2001) 447–452. [PubMed: 11694879]

[22]. Li S, Chen D, Sauve Y, McCandless J, Chen YJ, Chen CK, Rhodopsin-iCre transgenic mouse line for Cre-mediated rod-specific gene targeting, Genesis., 41 (2005) 73–80. [PubMed: 15682388]

[23]. Sanz E, Yang L, Su T, Morris DR, McKnight GS, Amieux PS, Cell-type-specific isolation of ribosome-associated mRNA from complex tissues, Proceedings of the National Academy of Sciences of the United States of America, 106 (2009) 13939–13944. [PubMed: 19666516]

[24]. Cleuren ACA, van der Ent MA, Jiang H, Hunker KL, Yee A, Siemieniak DR, Molema G, Aird WC, Ganesh SK, Ginsburg D, The in vivo endothelial cell translatome is highly heterogeneous across vascular beds, Proceedings of the National Academy of Sciences of the United States of America, 116 (2019) 23618–23624. [PubMed: 31712416]

[25]. Roh HC, Tsai LT, Lyubetskaya A, Tenen D, Kumari M, Rosen ED, Simultaneous Transcriptional and Epigenomic Profiling from Specific Cell Types within Heterogeneous Tissues In Vivo, Cell Rep, 18 (2017) 1048–1061. [PubMed: 28122230]

[26]. Widnell CC, Tata JR, A procedure for the isolation of enzymically active rat-liver nuclei, The Biochemical journal, 92 (1964) 313–317. [PubMed: 4284460]

[27]. Rajala A, McCauley A, Brush RS, Nguyen K, Rajala RVS, Phosphoinositide Lipids in Ocular Tissues, Biology (Basel), 9 (2020) 125. [PubMed: 32545642]

[28]. Rajala A, He F, Anderson RE, Wensel TG, Rajala RVS, Loss of Class III Phosphoinositide 3-Kinase Vps34 Results in Cone Degeneration, Biology (Basel), 9 (2020).

[29]. Dove SK, Piper RC, McEwen RK, Yu JW, King MC, Hughes DC, Thuring J, Holmes AB, Cooke FT, Michell RH, Parker PJ, Lemmon MA, Svp1p defines a family of phosphatidylinositol 3,5-bisphosphate effectors, Embo j, 23 (2004) 1922–1933. [PubMed: 15103325]

[30]. Menon M, Mohammadi S, Davila-Velderrain J, Goods BA, Cadwell TD, Xing Y, Stemmer-Rachamimov A, Shalek AK, Love JC, Kellis M, Hafler BP, Single-cell transcriptomic atlas of the human retina identifies cell types associated with age-related macular degeneration, Nat Commun, 10 (2019) 4902. [PubMed: 31653841]

[31]. Pauly D, Agarwal D, Dana N, Schäfer N, Biber J, Wunderlich KA, Jabri Y, Straub T, Zhang NR, Gautam AK, Weber BHF, Hauck SM, Kim M, Curcio CA, Stambolian D, Li M, Grosche A, Cell-Type-Specific Complement Expression in the Healthy and Diseased Retina, Cell reports, 29 (2019) 2835–2848.e2834. [PubMed: 31775049]

[32]. Carter-Dawson LD, LaVail MM, Rods and cones in the mouse retina. I. Structural analysis using light and electron microscopy, J.Comp Neurol, 188 (1979) 245–262. [PubMed: 500858]

[33]. Carter-Dawson LD, LaVail MM, Rods and cones in the mouse retina. II. Autoradiographic analysis of cell generation using tritiated thymidine, J.Comp Neurol, 188 (1979) 263–272. [PubMed: 500859]

[34]. Nikonov SS, Daniele LL, Zhu X, Craft CM, Swaroop A, Pugh EN Jr., Photoreceptors of Nrl −/− mice coexpress functional S- and M-cone opsins having distinct inactivation mechanisms, J.Gen.Physiol, 125 (2005) 287–304. [PubMed: 15738050]

[35]. Merlot S, Meili R, Pagliarini DJ, Maehama T, Dixon JE, Firtel RA, A PTEN-related 5-phosphatidylinositol phosphatase localized in the Golgi, J Biol Chem, 278 (2003) 39866–39873. [PubMed: 12878591]

[36]. Lees JA, Li P, Kumar N, Weisman LS, Reinisch KM, Insights into Lysosomal PI(3,5)P(2) Homeostasis from a Structural-Biochemical Analysis of the PIKfyve Lipid Kinase Complex, Mol Cell, 80 (2020) 736–743.e734. [PubMed: 33098764]

[37]. Hsuan J, Cockcroft S, The PITP family of phosphatidylinositol transfer proteins, Genome Biol, 2 (2001) Reviews3011. [PubMed: 11574064]

[38]. Ivanovic I, Allen DT, Dighe R, Le YZ, Anderson RE, Rajala RV, Phosphoinositide 3-kinase signaling in retinal rod photoreceptors, Invest Ophthalmol Vis Sci, 52 (2011) 6355–6362. [PubMed: 21730346]

[39]. Ivanovic I, Anderson RE, Le YZ, Fliesler SJ, Sherry DM, Rajala RV, Deletion of the p85alpha regulatory subunit of phosphoinositide 3-kinase in cone photoreceptor cells results in cone photoreceptor degeneration, Invest Ophthalmol Vis Sci, 52 (2011) 3775–3783. [PubMed: 21398281]

[40]. Nakatsu F, A Phosphoinositide Code for Primary Cilia, Dev Cell, 34 (2015) 379–380. [PubMed: 26305588]

[41]. Jin N, Chow CY, Liu L, Zolov SN, Bronson R, Davisson M, Petersen JL, Zhang Y, Park S, Duex JE, Goldowitz D, Meisler MH, Weisman LS, VAC14 nucleates a protein complex essential for the acute interconversion of PI3P and PI(3,5)P(2) in yeast and mouse, Embo j, 27 (2008) 3221–3234. [PubMed: 19037259]

[42]. Zhang Y, Zolov SN, Chow CY, Slutsky SG, Richardson SC, Piper RC, Yang B, Nau JJ, Westrick RJ, Morrison SJ, Meisler MH, Weisman LS, Loss of Vac14, a regulator of the signaling lipid phosphatidylinositol 3,5-bisphosphate, results in neurodegeneration in mice, Proceedings of the National Academy of Sciences of the United States of America, 104 (2007) 17518–17523. [PubMed: 17956977]

[43]. Chow CY, Zhang Y, Dowling JJ, Jin N, Adamska M, Shiga K, Szigeti K, Shy ME, Li J, Zhang X, Lupski JR, Weisman LS, Meisler MH, Mutation of FIG4 causes neurodegeneration in the pale tremor mouse and patients with CMT4J, Nature, 448 (2007) 68–72. [PubMed: 17572665]

[44]. Ungewickell A, Hugge C, Kisseleva M, Chang SC, Zou J, Feng Y, Galyov EE, Wilson M, Majerus PW, The identification and characterization of two phosphatidylinositol-4,5-bisphosphate 4-phosphatases, Proc.Natl.Acad.Sci U.S.A, 102 (2005) 18854–18859. [PubMed: 16365287]

[45]. Pendaries C, Tronchere H, Arbibe L, Mounier J, Gozani O, Cantley L, Fry MJ, Gaits-Iacovoni F, Sansonetti PJ, Payrastre B, PtdIns5P activates the host cell PI3-kinase/Akt pathway during Shigella flexneri infection, EMBO J., 25 (2006) 1024–1034. [PubMed: 16482216]

[46]. Li G, Anderson RE, Tomita H, Adler R, Liu X, Zack DJ, Rajala RV, Nonredundant role of Akt2 for neuroprotection of rod photoreceptor cells from light-induced cell death, J.Neurosci, 27 (2007) 203–211. [PubMed: 17202487]

[47]. Stilling S, Kalliakoudas T, Benninghoven-Frey H, Inoue T, Falkenburger BH, PIP(2) determines length and stability of primary cilia by balancing membrane turnovers, Communications biology, 5 (2022) 93. [PubMed: 35079141]

[48]. Ile KE, Kassen S, Cao C, Vihtehlic T, Shah SD, Mousley CJ, Alb JG Jr., Huijbregts RP, Stearns GW, Brockerhoff SE, Hyde DR, Bankaitis VA, Zebrafish class 1 phosphatidylinositol transfer proteins: PITPbeta and double cone cell outer segment integrity in retina, Traffic, 11 (2010) 1151–1167. [PubMed: 20545905]

[49]. Milligan SC, Alb JG Jr., Elagina RB, Bankaitis VA, Hyde DR, The phosphatidylinositol transfer protein domain of Drosophila retinal degeneration B protein is essential for photoreceptor cell survival and recovery from light stimulation, J Cell Biol, 139 (1997)351–363. [PubMed: 9334340]

[50]. Shang P, Stepicheva N, Teel K, McCauley A, Fitting CS, Hose S, Grebe R, Yazdankhah M, Ghosh S, Liu H, Strizhakova A, Weiss J, Bhutto IA, Lutty GA, Jayagopal A, Qian J, Sahel J-A, Samuel Zigler J, Handa JT, Sergeev Y, Rajala RVS, Watkins S, Sinha D, βA3/A1-crystallin regulates apical polarity and EGFR endocytosis in retinal pigmented epithelial cells, Communications biology, 4 (2021) 850. [PubMed: 34239035]

[51]. Chucair-Elliott AJ, Ocañas SR, Stanford DR, Ansere VA, Buettner KB, Porter H, Eliason NL, Reid JJ, Sharpe AL, Stout MB, Beckstead MJ, Miller BF, Richardson A, Freeman WM, Inducible cell-specific mouse models for paired epigenetic and transcriptomic studies of microglia and astroglia, Communications biology, 3 (2020) 693. [PubMed: 33214681]

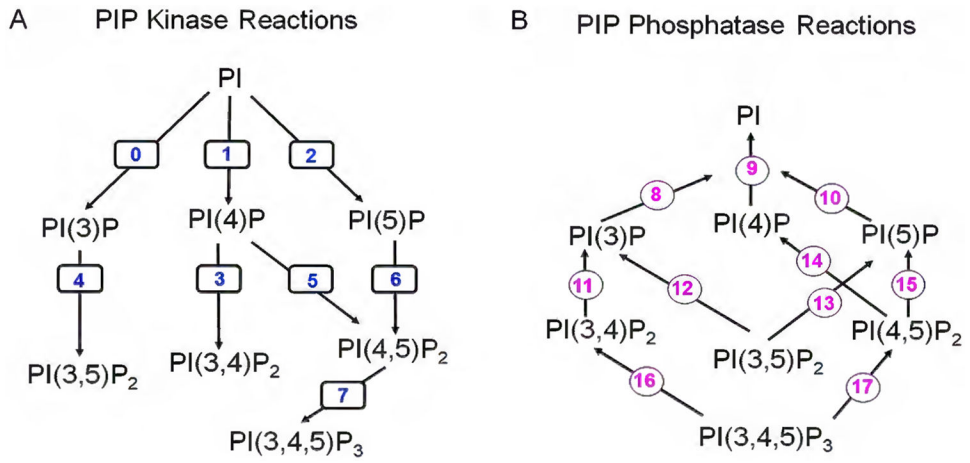

Figure 1. Generation of seven phosphoinositides by the action of PI kinases and PI phosphatases.

Kinase reactions are shown in panel **A**. Phosphatase reactions are shown in Panel **B**. Each kinase and phosphatase reaction is labeled with a number (0-17). **Kinase reactions: 0, 3, 7**— class I PI3K; **0, 3**—class II PI3K; **0**— Class III PI3K; **1**- PI4K IIα, PI4K IIβ, PI4K IIIα, PI4K IIIβ; **5**— PIPK 1α, PIPK Iβ, PIPK Iγ; **6**— PIPK IIα, PIPK IIβ, PIPK IIγ; **2, 4**—PIPK III (PIKFyve). **Phosphatase reactions: 8, 17**— PTEN; **13,17**—TPIP; **8,13**—MTM1; MTMR1, MTMR2, MTMR3, MTMR4, MTMR6, MTMR7, MTMR14, **8**—MTMR8; **11**— INPP4A, INPP4B; **15**—TMEM55A, TMEM55B; **8,9,12,14,15,16**—SYNJ1, SYNJ2; **14,16**—OCRL1, INPP5F, INPP5J, SKIP; **14,18**—INPP5B; **16**-SHIP1, SHIP2; **12,14,16**—INPP5E; **10**—PTPMT1; **8,9,12**—SACMIL; **12**—FIG4.

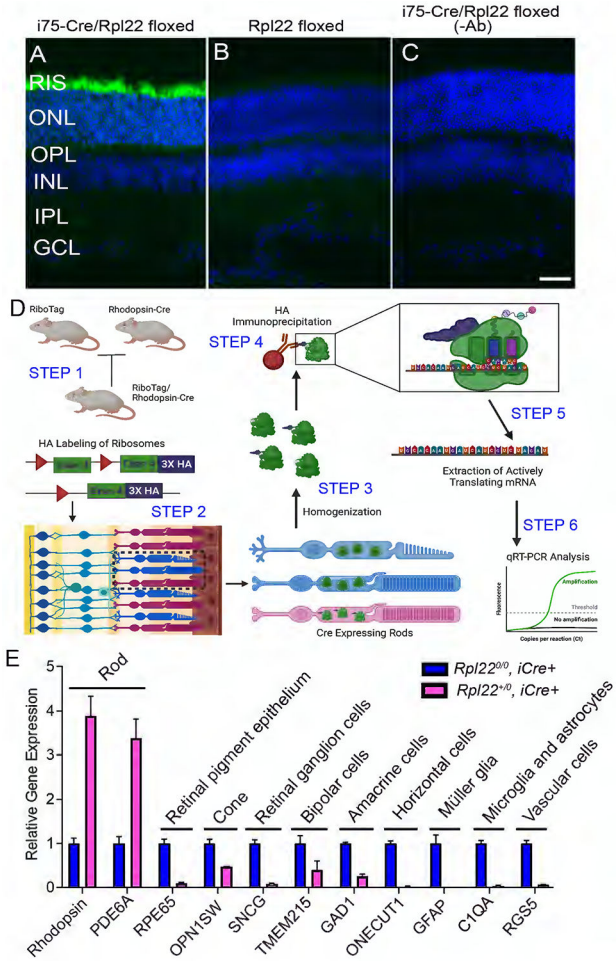

Figure 2. Cre-mediated activation of HA-tagged ribosomal protein in rod photoreceptor cells.

Retinal sections from i75-Cre/Rpl22 (**A**) and Rpl22 floxed (**B**) mice were stained with anti-HA antibody. Omission of HA antibody (**C**). Schematic diagram of RiboTag technique **(D)**. **Step 1:** Breeding rod-Cre mice with floxed *Rpl22* mice. **Step 2:** Cre-mediated expression of HA-tagged *Rpl22* protein. **Step 3:** Homogenization of retinas. **Step 4**: Incubation with HA antibody followed by Protein G-magnetic separation. **Step 5**: Isolation of RNA and synthesis of first-strand cDNA. **Step 6**: qRT-PCR with gene-specific primers. qRT-PCR analysis with various retinal cell-specific markers (**E**). Rod (rhodopsin, PDE6A), retinal pigment epithelium (RPE65), cone (OPN1SW), retinal ganglion cells (SNCG), bipolar cells (TMEM215), amacrine cells (GAD1), horizontal cells (ONECUT1), Müller glia (GFAP), microglia and astrocytes (C1QA), and vascular cells (RGS5). Data mean ± *SEM* (*n=3*). Panel **D** was created with BioRender.com.

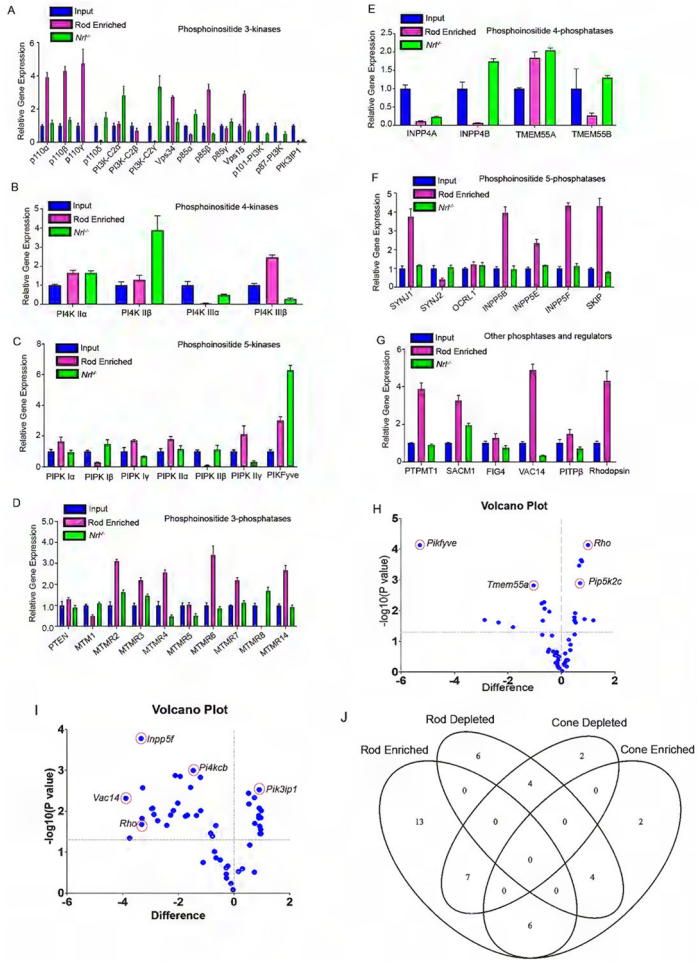

Figure 3. Gene expression of phosphoinositide kinases and phosphoinositide phosphatases in the retina (input), rods, and cones.

Equal amounts of mRNA from the retina, rods, and cones were used for quantitative real-time (RT)-PCR and normalized by β-actin levels. For clear representation, the data are presented as phosphoinositide 3-kinases (**A**), phosphoinositide 4-kinases (**B**), phosphoinositide 5-kinases (**C**), phosphoinositide 3-phosphatases (**D**), phosphoinositide 4-phosphatases (**E**), phosphoinositide 5-phosphatases (**F**), and other phosphatase and regulators (**G**). Rhodopsin was included as a reference (**G**). The mRNA levels were averaged and data were expressed as mean ± *SEM* (*n* = 3). Multiple unpaired *t*-tests were used to compare the differences between means. A significance level of $p<0.05$ was deemed significant. The volcano plot represents the combined data of both phosphoinositide kinases and phosphatases in the retina and cones (**H**). The plot is divided into three main categories: bottom, no significance; left upper, significantly increased in either retina compared with the cones or vice versa; the right upper significantly decreased in either retina compared with the cones or *vice versa*. The volcano plot represents the combined data of both phosphoinositide kinases and phosphatases (**I**) in the retina and rods. The plot is divided into three main categories: bottom, no significance; left upper, significantly increased in the rods compared with wild-type retina; the right upper, significantly decreased in the rods compared with wild-type retina. Using the R programming language, we generated a

Venn diagram (**J**) comparing the following four categories: (1) Cone-rich transcripts, which were significantly enriched in the cones; (2) Cone-poor transcripts, which were significantly decreased in the cones; (3) Rod-rich transcripts, which were significantly enriched in *Rpl22* isolates; and (4) Rod-poor transcripts, which were significantly decreased in *Rpl22* isolates.

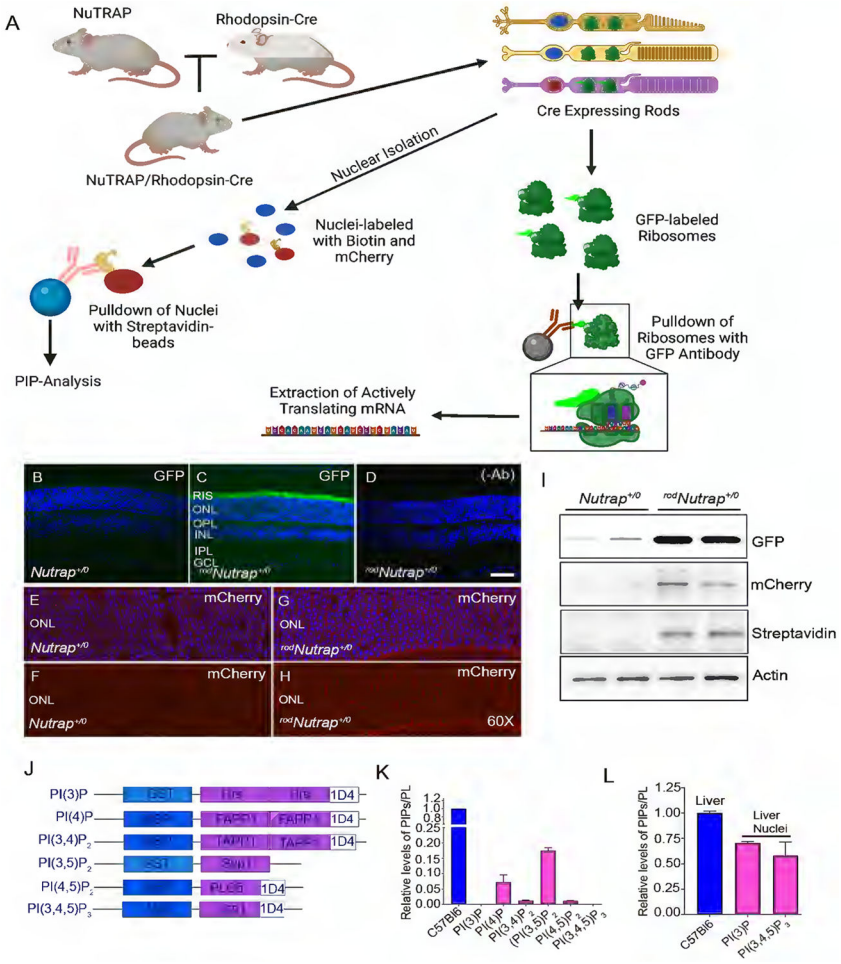

Figure 4. Cre-mediated labeling of nuclei with biotin and mCherry and ribosomes with GFP in rod photoreceptor cells.

Scheme of NuTRAP mouse line. Upon expression of Cre recombinase under the control of rhodopsin promoter, biotin and mCherry label nuclei and GFP enables tagging of the translating mRNA polysome complex (**A**). Retinal sections from *Nutrap*$^{+/0}$ and ^{rod}*Nutrap*$^{+/0}$ mice were stained with anti-GFP (**B, C**) and anti-mCherry (**E-H**) antibodies. Panel **D** is the omission of the GFP antibody. Panels **E** and **G** are stained with DAPI and mCherry antibody. Panels **F** and **H** are the same as **E** and **G** without DAPI. Immunoblot analysis of retinal proteins from *Nutrap*$^{+/0}$ and ^{rod}*Nutrap*$^{+/0}$ mice probed with anti-GFP, anti-mCherry, anti-streptavidin, and anti-actin antibodies (**I**). PIP probes are used to analyze PIPs (**J**). PIPs were measured from rod nuclei (**K**). Phosphoinositides were extracted from the mouse liver and mouse liver nuclei and we measured PI(3)P and PI(3,4,5)P_3 levels (**L**). Data are mean ± *SEM*, (*n=3*). Panel **A** was created with BioRender.com.

Table 1:

Retina cell type-specific primers for qRT-PCR

Cell type	Protein	Gene name	Forward primer	Reverse primer
Photoreceptor cells	Rhodopsin	*RHO*	CAAGAATCCACTGGGAGATGA	GTGTGTGGGGACAGGAGAACT
	Rod cGMP-specific 3',5'-cyclic phosphodiesterase subunit alpha	*PDE6A*	TCCTTGGGAGCAGCTAAAGG	CCTTCCCCCGGTAGTGAAAG
Cone photoreceptor cells	Short-wave length cone opsin	*OPN1SW*	TTTGGTCGCCATGTTTGTGC	AAAAGGGTGGGATGGACACC
Retinal pigment epithelium	RPE65	*RPE65*	GTTCCCCTGCAGTGATCGTT	GCAACATGAAGCCAAACCCC
Retinal ganglion cells	Gamma synuclein	*SNCG*	CCACAAGTCCACACACGCTA	ACAGCAGCATCTGATTGGTGA
Bipolar cells	Transmembrane protein 215	*TMEM215*	GGCAGGAGCCTTCAGGTAAC	ATGTCATCAGGCCGCATCTT
Amacrine cells	Glutamate decarboxylase 1	*GAD1*	CCGGATCTCTCCCTTCTTCAG	GTGGTCTTGGGGTCTCTACG
Horizontal cells	One Cut Homeobox 1	*ONECUT1*	GCAACGTGAGCGGTAGTTTC	CAAAGCCATTTGGGGTGAGC
Müller glia	Glial Fibrillary Acidic Protein	*GFAP*	CAGCCTCAGGTTGGTTTCAT	CTCTCCTGTGCTGGCTACTGT
Microglia and astrocytes	Complement C1qA	*C1QA*	CAAGGGGCTCTTTCAGGTGT	GTAAATGCGACCCTTTGCGG
Vascular cells	Regulator of G-protein signaling 5	*RGS5*	TCAAAATGGCGGAGAAGGCA	GACGGTTCCACCAGGTTCTT
Cytoskeletal protein	Actin	*ACTB*	ACTGGGACGACATGGAGAAG	GGGGTGTTGAAGGTCTCAAA

Table 2:

Primers for phosphoinositide kinases for qRT-PCR

Phosphoinositide 3-kinases	Protein	Gene name	Forward primer	Reverse primer
	p110α	*Pik3ca*	CACGATGTGAGCGGAAAGAG	AGATGGTCGTGGAGGCATTG
	p110β	*Pik3cb*	GGCATGCGGGTGTCGGA	ATAAATCCCGGTGGGCAGAAG
	p110δ	*Pik3cd*	GGGCCGAAAAGTGAATGCTG	AGCAAATAGAGCATCTGGGACAG
	P110γ	*Pik3cg*	TGGATCCATTGCCGGTTCAA	GGTGGGCAGTACGAACTCAA
	PI3K-C2α	*Pik3c2a*	CAGCGTGAGGTCCTGGTATT	CGAAGGGCTCAGAACAGGAG
	PI3K-C2β	*Pik3c2b*	CGCGCTATTGTCTCACCCG	TGGAAGACATGATGAGGGCG
	PI3K-C2γ	*Pikc2g*	GCCAGTTGATCCTGAGCCTT	CAGGTTGCTGTGTGTCTTGC
	Vps34	*Pik3c3*	TACCTGAACGTGATGAGGCG	AGCGCATGACTCTCACAGAC
	p85α	*Pik3r1*	GGAGAGAGCAGGCAAATTAAACA	TCCTTGGCTTTGCTCGGTT
	p85β	*Pik3r2*	CCCTACAGGCACTTGGTGTG	TGGGAGTATGTGGCCTGACT
	p85γ	*Pik3r3*	GACTTGTACTGGCCGTTGGA	AGGGGCTCAGAGAAGCCATA
	Vps15	*Pik3r4*	ATCGCCAGCTTGTTCAGACA	CAGTCATCCCCTGTGAGAGC
	pl01-PI3K	*Pik3r5*	CTCACCCCAACTGCTGAGAGTC	CAGTGGAACTTCGGTGGCTC
	p87-PI3K-adapter	*Pik3r6*	GACAGTGGAATTGAGCGGGA	GCCCTAGCATCCTGTCATCC
	PI3K-interacting protein 1 (inhibitor)	*PI3K1P1*	CTGAAAAACACCTCGGCTGC	CATCCTCGTCTCTTCGGCTC
Phosphoinositide 4-kinases	PI4K IIα	*Pik4k2a*	GCCCCATCTTGACAATCCCA	TCCCCCAAAGGAAACTGGAC
	PI4K IIβ	*Pik42b*	CCGCACTACGAGCTCAGAAA	ACTTCCACTTGACCCTTGAGA
	PI4K IIIα	*Pik4ca*	CACCTCCTGTCTCAGGTTCAA	TTACCTCTGCCTTTCCGAGC
	PI4K IIIβ	*Pik4cb*	GGCAACCGGCTCTTCTACTT	CGGACAGGGGAACTGAATGAA
Phosphoinositide 5-kinases	PIPK 1α	*Pip5k1a*	CGCAATACCGGGGTTTCCTT	CCGCGTCTCGGATAGAACAA
	PIPK Iβ (PIP5K1B)	*Pip5k1b*	GAGAACCCACGACATCCCGA	CAGGTACGGCGTCTCCATTT
	PIPK Iγ (PIP5K1C)	*Pip5k1c*	CACGGCCATGGAGTCTATCC	GAACTCTTCCGGAACACCGT
	PIPK IIα (PIP5K2A)	*Pip4k2a*	GCCACGTTCAAATCCCTGTC	GGGGTGCACTTCTGGTCAAG
	PIPK IIβ (PIP5K2B)	*Pip4k2b*	GCATGTCGTCCAACTGCACC	GGCCCGGAATAGCTTCACTT
	PIPK IIγ (PIP5K2C)	*Pip4k2c*	AGGACCTAAGCCTAAGCGGA	GAACAGTCGGGAACAGTCGT
	PIPK III (PIKFyve or PIP5K3)	*Pip5k3*	GATTCATCCGGATTCCTCAA	TAGCCTGGGGACTGACAGAT

Table 3:

Primers for phosphoinositide phosphatases for qRT-PCR

	Protein	Gene name	Forward primer	Reverse primer
Phosphoinositide 3-phosphatases	PTEN	*Pten*	GGAGCAAGGCTTGTAGTGGT	CCATTGGTAGCCAAACGGAAC
	TPIP	*Tpte2*	CAGAAGTGACCTGGAACAGAAA	CTGTGACATCACCGACATGGG
	MTM1	*Mtm1*	GAACTTACTGGCTGGTCAGG	GTGCCAGAGGAAAGGCATGT
	MTMR1	*Mtmr1*	CCTCCAGTTTCTCGCGCCAT	CCCGTGACCTAAAGGATGCC
	MTMR2	*Mtmr2*	GCTGGGAGCAGGTGGATAAA	CCCACAATTCCTGCAGTGGT
	MTMR3	Mtmr3	CGCCAAGGTAGAATGGGTGA	CTTGAGAGCCACTCTTGGCA
	MTMR4	Mtmr4	CCACATCTAGCTCTCGGCAG	GGACAAACCAACGGGCTTTC
	MTMR5	Mtmr5	CCACATCTAGCTCTCGGCAG	GGACAAACCAACGGGCTTTC
	MTMR6	*Mtmr6*	GGACAACCAAGGTTGAACAAGT	ATTGCATTGAGCTTGGGCCT
	MTMR7	*Mtmr7*	GAAAACGTGCGCTTGGTAGA	CGTGCAAGGCGTATCAGAGA
	MTMR8	*Mtmr8*	CCGTCAGACGCCGGT	GTACATCAGGGTGACCGAGT
	MTMR14	*Mtmr14*	AGGAGTTCTCCCGGACTCAG	CGGCCAAATAGCTCCAGACA
Phosphoinositide 4-phosphatases	INPP4A	*Inpp4a*	CCACGTGGTCCAAAAGCAAG	TTATGTTGCCGACACGGTCA
	INPP4B	*Inpp4b*	CACCGTGGAGAATAGGTCCG	TGGAGTACCTCGTCAGGGTC
	TMEM55A	*Tmem55a*	CGTACTTGCAGGAAAGCAGC	GGACATCCTATTCGCCGAGA
	TMEM55B	*Tmem55b*	ACGGAGCCGGTAAACATGC	CACAGATGACCCTGACACCC
Phosphoinositide 5-phosphatases	SYNJ1	*Synj1*	GGACGCTTCCTGAGCGGT	CCCCACACATGAGCCGTAAT
	SYNJ2	*Synj2*	CTGTGGGCCGAGCTATTGTC	CCCATTCAGAGCCGTCATCA
	OCRL1	*Ocrl*	ATTGGAGGCTTTGTGCCGAA	TAGGTAGCTGTCTTCTTCCAGGT
	INPP5B	*Inpp5b*	CTGAGACCGTAGGGACAGGA	CACAGGATTCGGTCACACCA
	SHIP1	*Inpp5d*	CCCCTGCATGGGAAATCAAC	TTTCCCAGATCCCCAGGTCT
	INPP5E	*Inpp5e*	AGGGGCATCCACTCTAGTCT	GGCAGGATTATGAAGTCCAGGG
	INPP5J	*Innpp5j*	CAGATCTCGCTGCCTACCTC	CTGCAACTGCTAACAAGTCAGG
	SAC2	*Inpp5f*	GGAGTCTCCTTGAGGCACGG	GTCTCCTGGGAGTTTGCCTAC
	SKIP	*Skip*	ATAAGCCTGTCACTGGCACC	GACGCATCCCCACCTTGTAT
Other	PLIP	*Ptpmt1*	GAAGCGATCGCCAAAATCCG	GGTCGGGTTAAGCTGCTTTG
	SAC1	*Sacm1l*	AGAGGTCACCCTTGCAGTCA	ACATCAAAATCTGTGGCTCTCCA
	SAC3	*Fig4*	GCTGGTTCATCGGGTAAAGA	GGCTCATGGTGTTTTTGTGA
	PITPβ	*PITPβ*	TCAGGTTGGACAGCTTTACTCT	GTGTACTGTCCCTTCTCGCC
	VAC14	*Vac14*	CTGCTGGACGTGAAGAACAAC	CTAGGGCCCTTTTCCATGCT

Table 4:

Mammalian phosphoinositide kinases

Class/type	Protein	Catalyzes the reaction	Gene name
Class IA PI3K	p110α	**0, 3, 7**	*Pik3ca*
	p110β	**0, 3, 7**	*Pik3cb*
	p110δ	**0, 3, 7**	*Pik3cd*
Regulatory subunits			
	p85α		*Pik3r1*
	p85β		*Pik3r2*
	p85γ		*Pik3r3*
	Vps15		*Pik3r4*
	p101-PI3K		*Pik3r5*
	p87-PI3K-adapter		*Pik3r6*
Class IB PI3K	p110γ	**0, 3, 7**	*Pik3cg*
Class II PI3K	PI3K-C2α	**0, 3**	*Pik3c2a*
	PI3K-C2β	**0, 3**	*Pik3c2b*
	PI3K-C2γ	**0, 3**	*Pikc2g*
Class III PI3K	Vps34	**0**	*Pik3c3*
Phosphatidylinositol 4-kinases			
Type II PI4Ks	PI4K IIα	**1**	*Pik4k2a*
	PI4K IIβ	**1**	*Pik42b*
Type III PI4Ks	PI4K IIIα	**1**	*Pik4ca*
	PI4K IIIβ	**1**	*Pik4cb*
Phosphatidylinositol phosphate kinases			
Type I PIPKs	PIPK 1α	**5**	*Pip5k1a*
	PIPK Iβ	**5**	*Pip5k1b*
	PIPK Iγ	**5**	*Pip5k1c*
Type II PIPKs	PIPK IIα	**6**	*Pip4k2a*
	PIPK IIβ	**6**	*Pip4k2b*
	PIPK IIγ	**6**	*Pip4k2c*
Type III PIPKs	PIPK III	**2, 4**	*Pip5k3*

Table 5:

Mammalian phosphoinositide phosphatases

Class/type	Protein	Catalyzes the reaction	Gene name
Phosphoinositide 3-phosphatases			
PTEN	PTEN	**8, 17**	*Pten*
TPIP	TPIP	**13, 17**	*Tpte2*
Myotubularins	MTM1	**8, 13**	*Mtm1*
	MTMR1	**8,13**	*Mtmr1*
	MTMR2	**8,13**	*Mtmr2*
	MTMR3	**8,13**	*Mtmr3*
	MTMR4	**8,13**	*Mtmr4*
	MTMR6	**8,13**	*Mtmr6*
	MTMR7	**8, 13**	*Mtmr7*
	MTMR8	**8**	*Mtmr8*
	MTMR14	**8,13**	*Mtmr14*
Phosphoinositide 4-phosphatases			
INPP4	INPP4A	**11**	*Inpp4a*
	INPP4B	**11**	*Inpp4b*
TMEM55	TMEM55A	**15**	*Tmem55a*
	TMEM55B	**15**	*Tmem55b*
Phosphoinositide 5-phosphatases			
Type II INPP5s	SYNJ1	**8,9,12,14,15,16**	*Synj1*
	SYNJ2	**8,9,12,14,15,16**	*Synj2*
	OCRL1	**14,16**	*Ocrl*
	INPP5B	**14,18**	*Inpp5b*
	INPP5J	**14,16**	*Inpp5j*
	SKIP	**14,16**	*Skip*
Type III INPP5s	SHIP1	**16**	*Inpp5d*
	SHIP2	**16**	*Inppl1*
Type IV INPP5	INPP5E	**12, 14,16**	*Inpp5e*
Others			
PLIP	PLIP	**10**	*Ptpmt1*
Sac	SAC1	**8, 9, 12**	*Sacm1l*
	SAC2	**14, 16**	*Inpp5f*
	SAC3	**12**	*Fig4*

Table 6.

Differential expression of PI converting enzymes between Rods and Cones.

Photoreceptor-Rich	Rod/Cone-Rich	*Pip5k3* *Mtmr2* *Mtmr3* *Pi4k2a* *Tmem55a* *Sacm1*
Photoreceptor-Poor	Rod/Cone-Poor	*Inpp4a* *Pi4kca* *Pik3r5* *Pik3ip1*
Rod-specific Enrichment	Rod-Rich/ Cone-Poor	*Pi4kcb* *Pik3r4* *Pik3r2* *Pik3cg* *Mtmr4* *Vac14* *Rhodopsin*
Cone-specific Enrichment	Rod-Poor/Cone-Rich	*Mtmr8* *Inpp4b* *Pik3r1* *Pik3c2y*